



Published in final edited form as:

ACS Nano. 2009 November 24; 3(11): 3447–3454. doi:10.1021/nn900884n.

## Modulating the Gelation Properties of Self-Assembling Peptide Amphiphiles

Joel M. Anderson<sup>†</sup>, Adinarayana Andukuri<sup>†</sup>, Dong Jin Lim<sup>†</sup>, and Ho-Wook Jun<sup>†,\*</sup>

<sup>†</sup> Department of Biomedical Engineering, University of Alabama at Birmingham, Birmingham, AL 35294-2182

### Abstract

Peptide amphiphiles (PAs) are self-assembling molecules that form interwoven nanofiber gel networks. They have gained lots of attention because of their excellent biocompatibility, adaptable peptide structure that allows for specific biochemical functionality, and nanofibrous assembly that mimics natural tissue formation. However, variations in molecule length, charge, and intermolecular bonding between different bioactive PAs cause contrasting mechanical properties. This potentially limits cell-delivery therapies because scaffold durability is needed to withstand the rigors of clinician handling and transport to wound implant sites. Additionally, the mechanical properties have critical influence on cellular behavior, as the elasticity and stiffness of biomaterials have been shown to affect cell spreading, migration, contraction, and differentiation. Several different PAs have been synthesized, each endowed with specific cellular adhesive ligands for directed biological response. We have investigated mechanical means for modulating and stabilizing the gelation properties of PA hydrogels in a controlled manner. A more stable, biologically-inert PA (PA-S) was synthesized and combined with each of the bioactive PAs. Molar ratio ( $M_r = PA/PA-S$ ) combinations of 3:1, 1:1, and 1:3 were tested. All PA composites were characterized by observed nanostructure and rheological analysis measuring viscoelasticity. It was found that the PAs could be combined to successfully control and stabilize the gelation properties, allowing for a mechanically-tunable scaffold with increased durability. Thus, the biological functionality and natural degradability of PAs can be provided in a more physiologically-relevant microenvironment using our composite approach to modulate the mechanical properties, thereby improving the vast potential for cell encapsulation and other tissue engineering applications.

### Keywords

Peptide amphiphile; hydrogel; viscoelasticity; biomimetic material; ECM (extracellular matrix)

---

With ever expanding research into synthetic biomaterials, the importance of recapitulating the innate characteristics of biological tissue microenvironments, including the biochemical and mechanical properties, has gained greater importance. In particular, synthetic microenvironments need to provide both the spatial and temporal complexities necessary to guide cell-specific tissue development and function.<sup>1</sup> Peptide-based hydrogels offer one such promising biomaterial, crafted to simplistically mimic the native extracellular matrix (ECM).

---

\*Corresponding author: Dr. Ho-Wook Jun; hwjun@uab.edu; University of Alabama at Birmingham, Shelby 806, 1825 University Blvd., Birmingham, AL 35294-2182, United States; office: 205-996-6938; fax: 205-974-6938.

**Supporting Information Available:** (1) Macroscopic gelation properties of peptide amphiphile composite hydrogels modulated at a 3:1 molar ratio. (2) Viscoelastic characterization using dynamic oscillatory rheometry to measure storage modulus in relation to frequency for peptide amphiphile composite hydrogels modulated at a 3:1 molar ratio. This material is available free of charge via the Internet at <http://pubs.acs.org>.

The ECM is vital for directing cell fate processes, as many different amino acid ligands are presented in the dynamic network of collagens, proteoglycans, and adhesion proteins.<sup>2</sup> Capturing these biological cues within peptide-based biomaterials holds great promise for controlling many tissue specific cell-ECM interactions, which initiate intercellular signaling pathways such as adhesion, proliferation, migration, and differentiation.<sup>3</sup> In addition to directing the cellular response, the mechanical properties of three-dimensional hydrogels must also be explored in depth to completely mimic the ECM microenvironment. Hence, the modulation of mechanical properties within peptide-based hydrogels has been investigated for this study.

Polymer hydrogels commonly synthesized from materials such as polyethylene glycol can be easily modified with peptides and have been frequently studied.<sup>4-6</sup> These types of polymer hydrogels allow for strong gelation control. However, they are typically crosslinked into gel networks by ultraviolet or redox initiation, thereby presenting cytotoxicity concerns for cell encapsulation.<sup>7</sup> Other classes of peptide-based hydrogels include biomaterials that can naturally self-assemble into nanofibrous gels. For example, Zhang and coworkers have developed a peptide hydrogel characterized by alternating hydrophobic and hydrophilic residues, which is induced to self-assemble by changing the pH.<sup>8-10</sup> Peptide amphiphiles (PAs) are also prevalently used as peptide-based hydrogels, offering inherent biocompatibility, versatility within the internal peptide structure, natural degradability, and easily accessible bioactivity. However, these types of self-assembling biomaterials often present difficulties for precisely controlling the gelation and mechanical properties. Therefore, methods to modulate the mechanical properties of PA hydrogels have been investigated for this study.

PAs are self-assembling molecules with a very adaptable composition that allows for the concurrent control of nanostructure and biochemical functionality.<sup>11</sup> The general structure consists of a hydrophilic peptide segment attached via an amide bond to a hydrophobic aliphatic tail.<sup>12</sup> The self-assembly of PAs into nanofibers can be induced by lowering the pH or adding multivalent ions.<sup>13</sup> Driven by the molecular shape and amphipathic nature, the self-assembled PAs configure into a cylindrical micelle nanofibers; each with a highly packed hydrophobic core of radially aligned alkyl tails and peptide regions exposed to the outside.<sup>12, 14, 15</sup> A viscoelastic three-dimensional hydrogel is formed when a sufficient concentration between the interwoven nanofibers is reached.<sup>16, 17</sup> The applications for PAs are far-reaching and include such uses as nanoelectronics, drug delivery, tissue engineering.<sup>18</sup> Moreover, PAs have been studied as a biomaterial across many different cell and tissue types, including osteogenic, neuronal, and dental lineages.<sup>19-25</sup> However, in the current landscape, stability issues limit the clinical practicality of self-assembled PA gels because of concerns for clinician handling and the durability of cell-loaded scaffolds after implantation for wound regeneration.<sup>26</sup> In addition to stability needs, precise control of the PA gelation properties is critical for influencing cellular behaviors, as recent literature has shown that the mechanical properties of biomaterials, such as elasticity and stiffness, directly affect cell spreading, migration, contraction, organization of intracellular structures, and differentiation.<sup>27-29</sup> Therefore, more attention to the gelation properties is warranted, particularly the need to better define and control the three-dimensional environment through mechanical modulation.

Previous means to modulate the mechanical properties of peptide-based hydrogels include phospholipid inclusions and chemical ligation. Paramonov *et al.* successfully combined PA nanofibers with phospholipids at the optimal ratio to maximize the storage modulus.<sup>30</sup> Jung *et al.* were able to manipulate the stiffness of self-assembling peptide hydrogels by chemically producing bonds between the termini of the fibrillized  $\beta$ -sheet peptides.<sup>31</sup> However, a composite system that combines multiple PAs to modulate the gelation mechanical properties has yet to be fully investigated. Previously, the main efforts to combine two distinct PAs focused on self-

assembly mechanisms using binding electrostatic attraction or polarity, but no mechanical evaluations were performed.<sup>32–34</sup>

We propose to combine two functionally-specific PAs with differing mechanical properties to create a composite system. This approach would allow for increased stability, easy optimization, and provide the greater control needed for creating cell encapsulating microenvironments within the ECM-mimicking gels. Thus, the goal of this study is to control the mechanical properties of self-assembled PA hydrogels using a simple mixing approach to obtain the necessary stability and practicality. In particular, we aim to ensure that stability is maintained across many different PA sequences, provide an unbiased starting point for potential cellular evaluations by bestowing comparable mechanical properties despite containing differing peptide ligands, and impart the corresponding stiffness and viscoelasticity of native ECMs. For this study, different PA molecules, each functionalized with an isolated ligand sequence from the ECM, have been separately combined with a stronger gelating, non-biologically active PA molecule (PA-S) at different molar ratios ( $M_r = PA/PA-S$ ). To be combined with PA-S, four different bioactive PAs, each inscribed with a specific ligand in the peptide headgroup, were synthesized to mimic the wide range of cell-ECM interactions. The functionalized PAs by themselves exhibit differing physical properties after gelation is induced because of the disparity in length, shape, and charge between the molecules.<sup>13, 17, 35</sup> Consequently, the design of our adaptable system is to control these variations by introducing the stronger PA-S in combination with the functionalized PAs to better regulate the mechanical environment and achieve practical stability of the self-assembled gels, while still maintaining the presence of the specific biological functionality.

Including the non-biologically active PA-S, five different PAs were synthesized for this study. The basic PA structure of each can be divided into three regions, consisting of a functional ligand site, enzyme-cleavable sequence sensitive to matrix metalloproteinase-2 (MMP-2), and hydrophobic aliphatic tail. The PA organization remained the same for all molecules, except for PA-S, which did not include an isolated ligand motif. The four different ligands separately inscribed into PAs encompassed a broad scope of cell-ECM interactions and included the following peptide sequences: (1) Arg-Gly-Asp-Ser (RGDS), (2) Val-Ala-Pro-Gly (VAPG), (3) Asp-Gly-Glu-Ala (DGEA), and (4) Tyr-Ile-Gly-Ser-Arg (YIGSR). RGDS is an integrin-mediated binding site found in many ECM molecules, such as fibronectin and laminin, and it has been well-established to increase general cell adhesion.<sup>36, 37</sup> VAPG is an elastin-derived sequence, specific for smooth muscle cell adhesion via non-integrin binding.<sup>38</sup> DGEA is an adhesive ligand for collagen type I, interacting with osteoblasts through the  $\alpha_2\beta_1$  integrin receptor.<sup>39</sup> The YIGSR moiety is isolated from laminin and has been found to influence endothelial cell attachment and morphology.<sup>40, 41</sup> The enzyme-cleavable sequence (Gly-Thr-Ala-Gly-Leu-Ile-Gly-Gln) was incorporated into all of the PAs, and its inclusion is essential for potential cell encapsulation studies because it enables cell migration and ECM remodeling within the PA network.<sup>17</sup> Each of the functionalized PAs (i.e. PA-RGDS, PA-VAPG, PA-DGEA, PA-YIGSR) was mixed with PA-S at molar ratios ( $M_r = PA/PA-S$ ) of 3:1, 1:1, and 1:3 to modulate the mechanical properties of the self-assembling gels as shown in Scheme 1. The nanostructure formations were observed under transmission electron microscope (TEM) imaging. The gelation performance, including viscoelasticity, was evaluated by dynamic oscillatory rheometry.

## Results and Discussion

All five PAs were synthesized and verified to have the correct molecular weight values as follows: PA-RGDS [ $CH_3(CH_2)_{14}CONH-GTAGLIGQ-RGDS$ ; MW = 1369.97], PA-VAPG [ $CH_3(CH_2)_{14}CONH-GTAGLIGQ-VAPG$ ; MW = 1278.97], PA-DGEA [ $CH_3(CH_2)_{14}CONH-GTAGLIGQ-DGEA$ ; MW = 1326.92], PA-YIGSR [ $CH_3(CH_2)_{14}CONH-GTAGLIGQ-$

YIGSR; MW = 1531.09], and PA-S [ $\text{CH}_3(\text{CH}_2)_{14}\text{CONH-GTAGLIGQ-S}$ ; MW = 1041.82]. The nanostructure of each PA was characterized by TEM imaging after adding divalent calcium ions to induce nanofiber self-assembly (Figure 1). Despite differences in chemical composition and sequence length, each of the PAs self-assembled into uniform nanofiber networks with nanoscopic diameters (~10 nm) and extended lengths approaching several microns. This qualitatively confirms successful self-assembly similar to previous PA hydrogel studies.<sup>12, 16, 17</sup>

The mechanical properties of the individual PAs were next analyzed by dynamic oscillatory rheometry. The oscillatory tests were performed at variable frequencies, providing dynamic mechanical analysis of the storage moduli ( $G'$ ). The storage modulus is an indicator of elastic behavior and measures the ability to store deformation energy that can be recovered after removing the load cycle.<sup>42</sup> As shown in Figure 2, a diverse spectrum of storage modulus values was observed for the different PAs after induced self-assembly. The PA-S hydrogel had the highest storage modulus, exhibiting strong gelation properties at least 2–3 times greater than the other PAs. The PA-RGDS and PA-VAPG hydrogels followed behind PA-S with storage moduli approaching 150 pascals (Pa). The two remaining gels of PA-DGEA and PA-YIGSR demonstrated minimal storage modulus values that were close to zero. In general, a certain gel stability can be assumed if  $G' \geq 10$  Pa; however, stability in relation to practical use is almost always lacking if  $G' \leq 1$  Pa.<sup>43</sup> Thus, the same mechanical properties in regard to viscoelasticity are not maintained across all the PAs, fluctuating as different cell adhesive ligand sequences are incorporated and limiting the potential applicability.

These differences are further demonstrated by visual inspection of the macroscopic PA gels as depicted in Table 1. The physical gelation of each PA varied in the same manner as observed under oscillatory rheometry. After inducing self-assembly, moderately stable hydrogels were formed with PA-RGDS and PA-VAPG, only viscous solutions resulted for PA-DGEA and PA-YIGSR, and PA-S displayed the strongest gel character. Among the bioactive PAs, the moderate hydrogels offer potential for cell encapsulation and other tissue engineering applications, but no such practical claim can be justified for the PAs that only self-assembled into viscous solutions. Therefore, PA-S was mixed with each of the PAs at molar ratios ( $M_r = \text{PA}/\text{PA-S}$ ) of 3:1, 1:1, 1:3 to improve and better control the gelation parameters. The 3:1 molar ratio combination did not produce any major changes in the physical appearance of the PA hydrogels (see Supporting Information). However, the gelation character was greatly improved for all PA mixtures at both 1:1 and 1:3 molar ratios. Each of the composite PAs self-assembled into much more structurally stable gels with a better defined cylindrical shape and increased durability for handling and transport.

TEM imaging of the nanostructure was again performed to ensure that each of the composite PAs still retained a consistent nanofibrous network (Figure 3). In all cases, the nanoscopic appearances for the PAs self-assembled with PA-S ( $M_r = 1:1$  and 1:3) were comparable to previous observations involving only one PA sequence. While the nanostructure remained unchanged, the viscoelastic properties of the composite PA hydrogels were drastically altered as evaluated by dynamic oscillatory rheometry (Figure 4). Two subsets of mechanically similar PA hydrogels were created at  $M_r = 1:1$ , and all of the composites were stabilized to the same relative storage modulus at  $M_r = 1:3$ . For the  $M_r = 1:1$  hydrogels, PA-RGDS and PA-VAPG both exhibited approximately the same storage modulus ( $G' \approx 150$  Pa), and the previously viscous solutions of PA-DGEA and PA-YIGSR had greatly improved their viscoelasticity ( $G' \approx 50$  Pa). Additionally, the storage moduli for all of the composite PAs became in sync at the 1:3 molar ratio. Within this molar combination, the values for PA-RGDS and PA-VAPG remained unchanged, while the storage modulus for both PA-DGEA and PA-YIGSR increased to meet the same level.

To further illustrate the modulating of mechanical gelation properties using this composite approach, the ratio of storage modulus to loss modulus was compared for all PA combinations at the molar ratios ( $M_r = \text{PA-S/PA}$ ) of 1:0, 3:1, 1:1, and 1:3 (Table 2). The loss modulus ( $G''$ ) is a measure of deformation energy dissipated as heat and friction during the shearing process.<sup>43</sup> A ratio of storage modulus to loss modulus ( $G'/G''$ ) greater than one is commonly used to indicate gel formation.<sup>44</sup> As shown in Table 2, the  $G'/G''$  ratios trended upward as the fraction of PA-S in the composite hydrogels increased. The  $G'/G''$  ratios for both PA-RGDS and PA-VAPG increased gradually from  $M_r = 1:0$  to  $M_r = 1:1$ , but there was a generally larger jump at  $M_r = 1:3$ . Conversely, a large increase in the  $G'/G''$  ratios for PA-DGEA and PA-YIGSR was first detected at  $M_r = 1:1$ , corresponding to the rapid improvement in the macroscopic gel quality.

While a ratio of  $G'/G'' \geq 1$  has often been used to define technical gel formation, it is very evident from these studies that this rationale cannot be relied upon exclusively. PA-DGEA and PA-YIGSR both exhibited  $G'/G''$  ratios exceeding one at every molar combination, but only stable gel formations were observed at  $M_r = 1:1$  and 1:3. Thus, the physical appearance and durability of the PA hydrogels must be the deciding factor to ensure that the requisite level of practical gel stability is achieved for biomedical applications. However, the  $G'/G''$  ratio still has some merit as a gelation indicator because the observed values did rise as the fraction of PA-S increased, displaying the highest ratios at  $M_r = 1:3$  for all hydrogels.

The mechanisms behind PA-S demonstrating stronger gelation mechanical properties are not fully understood. It is believed that the lack of a ligand sequence in the outer domain of PA-S allows for self-assembly into a hydrogel with stronger mechanical properties because the core interactions between the peptide monomers are not weakened by extended peptide chains necessitated by the inclusion of functional ligand motifs. This phenomenon is believed to occur because the amino acids closest to the hydrophobic nanofiber core have been shown as the most critical for forming higher order PA assemblies.<sup>14</sup> While the molecular length and critical bonding between the core amino acids definitely affect the self-assembly interactions, several other variables may also factor into the gelation process. Within the PA composition, the hydrophobicity, bulkiness, and conformational flexibility of the amino acids have all been shown to affect PA gel character.<sup>45</sup> Also, the surrounding local environment, properties of the counter ions (e.g. concentration, valence), and intermolecular forces all significantly factor into the self-assembly kinetics and gel mechanical properties for PAs.<sup>14, 15</sup> Regardless, the resulting effect of controlling the mechanical modulation of peptide-based hydrogels has many potential benefits for tissue regenerative treatments.

All of the different PA mixtures were found to self-assemble into nanofiber networks after adding calcium. Based on the TEM imaging, it is unclear if the PA composites consisted of two distinctly separate nanofibers or as mixed nanofibers in which the bioactive PAs and PA-S molecules self-assembled within the same structures. Previous literature, however, strongly suggests that a homogenous mixture occurs and that the PA molecules are not mutually exclusive during composite nanofiber self-assembly.<sup>32, 33</sup> In any case, the nature of self-assembly within this composite approach is not believed to limit the functionality of the bioactive PAs, while the added benefit of a more tunable nanomatrix is gained.

The ECM produces many different mechanical environments that vary according to tissue, resulting in altered force levels within the cell-ECM adhesions that produce changes in the intracellular biochemistry and govern cell fate.<sup>46</sup> Therefore, controlling the mechanical properties of peptide-based hydrogels is crucial for developing an instructive cellular microenvironment that mimics the natural ECM. By employing our composite approach, PAs can be modulated to serve as a scaffold for many different cell types by matching the mechanical properties required for the desired tissue engineering application. This is of

particular importance for culturing stem cells within the PA hydrogels because Engler *et al.* has shown that stem cell lineage specification can be directed by changing the substrate elasticity to correlate the matrix stiffness to native ECM stiffness.<sup>47, 48</sup> Additionally, the ligand density presented by the two combined PAs could potentially be controlled by altering the mixture ratios. This will allow for even greater biological control within the PA composites because the density and spatial arrangement of ligand signals are central for guiding the localized cellular responses.<sup>49–52</sup>

Overall, the modulation of PAs by combining two sequences has great potential for many future tissue-specific cell encapsulation and injection studies. By merging bioactive and mechanical properties, the adhesive ligand signaling can be maintained while still providing the most biomimetic surroundings. The other added benefits include a more durable PA hydrogel that is able to withstand the rigors of clinician handling for transport and implantation at traumatized wound sites via *in situ* formation or injection delivery. Also, PAs functionalized with different ligand moieties can be evaluated together under the same mechanical conditions after adjusting with the stronger, biologically-inert PA, thereby evaluating the cell-responsive signals on their merit alone and without mechanical variation. This will provide a biologically relevant comparison between the PA hydrogels and natural tissue microenvironments.

## Conclusion

PAs offer a very versatile biomaterial that is capable of biochemical adaptation to support many types of cells and tissues by interchanging peptide adhesive ligands sequences within the internal structure. To better facilitate and promote cell-based therapies, however, the nanofibrous PA microenvironment must also provide the same physical environment as native tissue and ECM. Previously, this has proven difficult because varying mechanical properties result after inducing hydrogel self-assembly of PAs inscribed with different cell-specific ligands. Consequently, while capable of invoking specific bioresponsive activity based on the cellular adhesive ligands, the PAs are often lacking in practical stability and the durability needed for cell-loading, handling, and transport. To overcome these limitations, this study modulated the mechanical properties by combining biologically-functionalized PAs with a stronger, biologically-inert PA. It was found that the viscoelasticity and overall gel character could be directly controlled and stabilized by adjusting the molar ratio fraction between both PA molecules. Therefore, this composite approach allows for the simultaneous control of bioactivity and mechanical properties within PA hydrogels, which will be vitally important for the continued development of biomaterial regenerative strategies.

## Materials and Methods

### Peptide amphiphile synthesis

All peptide sequences were synthesized using standard Fmoc-chemistry on an Advanced Chemtech Apex 396 peptide synthesizer as described previously.<sup>17, 19, 53, 54</sup> Briefly, the peptides were alkylated at the *N*-termini with palmitic acid in a mixture of *o*-benzotriazole-*N,N,N',N'*-tetramethyluroniumhexafluorophosphate (HBTU), diisopropylethylamine (DiEA), and dimethylformamide (DMF). Alkylation was performed twice for two 12 hour intervals at room temperature. Cleavage and deprotection followed for 3 hours, using a mixture of trifluoroacetic acid (TFA), deionized (DI) water, triisopropylsilane, and anisole (40:1:1:1). The collected samples were rotoevaporated to remove excess TFA, precipitated in ether, and dried under vacuum using lyophilization. Successful PA syntheses were confirmed by matrix-assisted laser desorption ionization time of flight (MALDI-TOF) mass spectrometry.

### Self-assembly of peptide amphiphile gels

For each PA, 2% (weight/volume) stock solutions were prepared and buffered to neutral pH (~7) with NaOH. The functionalized PAs (i.e. PA-RGDS, PA-VAPG, PA-DGEA, PA-YIGSR) and non-biologically active PA-S were prepared to be individually self-assembled. Additionally, different PA combinations were prepared between the functionalized PAs and biologically-inert PA-S based on molar ratios ( $M_r = \text{PA}/\text{PA-S}$ ) of 3:1, 1:1, 1:3. Self-assembly for all PAs, including the mixed solutions, was induced by combining 50  $\mu\text{L}$  of PA solution with 50  $\mu\text{L}$  of deionized (DI) water containing 0.1 M  $\text{CaCl}_2$  in 12-well silicone flexiPERM cell-culture chambers attached to glass coverslips. The molar ratio between PA and calcium ions ( $M_r = \text{Ca}^{2+}/\text{PA}$ ) was held constant at  $M_r = 2$  for all self-assembled gels.

### TEM imaging of peptide amphiphiles

The different PA combinations were prepared and self-assembled as described in the previous section. A 5  $\mu\text{L}$  self-assembled sample was applied to a carbon coated formvar copper grid (400 mesh) for 1 minute. 10  $\mu\text{L}$  of 20% phosphotungstic acid (PTA) buffered to pH 7 were added to the grids for negative staining. The PTA solution was allowed to stain for 30 seconds before the excess was wicked off. The samples were examined on a Tecnai T12 microscope by FEI operated at 60 kV accelerating voltage.

### Rheological characterization

The viscoelastic properties of the PA hydrogels were analyzed on an AR 2000 Rheometer (TA Instruments, UK). All PA mixture combinations characterized were prepared as described previously. Dynamic oscillatory shear was measured on a flat-plate circular construct with 10 mm diameter. For each characterization, pre-shear was applied to obtain equilibrium. The storage modulus ( $G'$ ) and loss modulus ( $G''$ ) was evaluated over a wide frequency range (0.1 – 10 Hz) at 25°C.

### Supplementary Material

Refer to Web version on PubMed Central for supplementary material.

### Acknowledgments

The authors extend many thanks to thank Melissa Chimento for use of the High Resolution Imaging Facility, along with the Mass Spectrometry/Proteomics Shared Facility for measuring the molecular weights of all PA samples. Appreciation is also acknowledged to Dr. Derrick Dean for the use of his lab for all rheological characterizations. This work was supported by the Wallace H Coulter Foundation (HWJ), 2007 Intramural Pilot Grant from the BioMatrix Engineering and Regenerative Medicine Center at UAB (HWJ), NIH T32 predoctoral training grant (NIBIB #EB004312-01) for JMA, and Caroline P Ireland Research Scholarship (AA).

### References

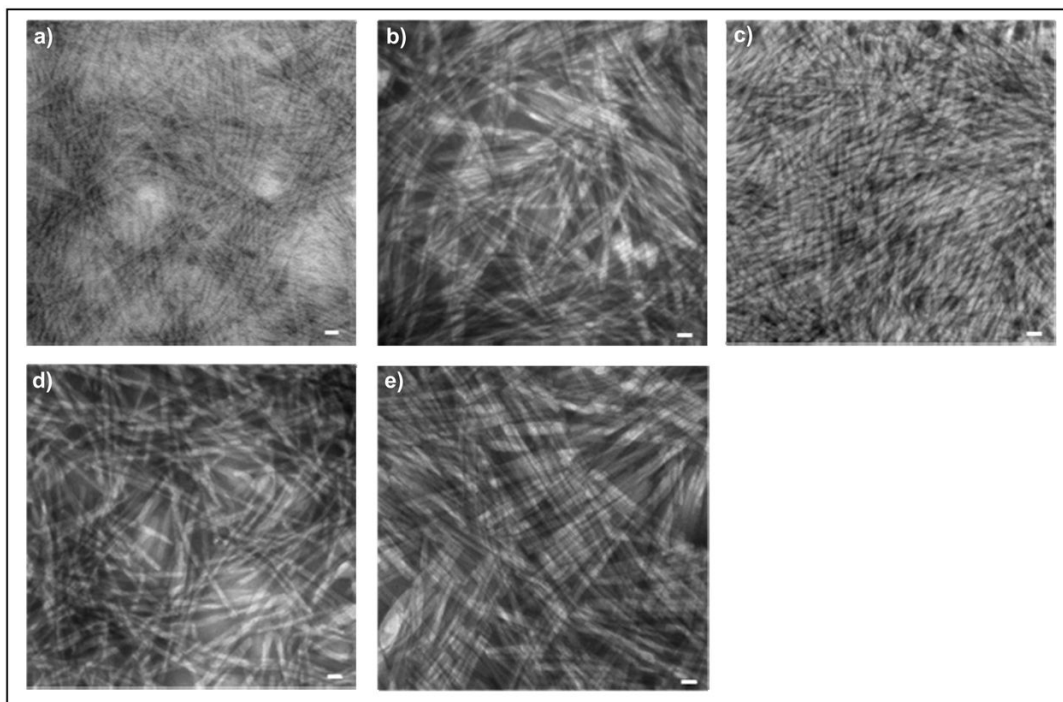
1. Lutolf MP, Hubbell JA. Synthetic Biomaterials as Instructive Extracellular Microenvironments for Morphogenesis in Tissue Engineering. *Nat Biotechnol* 2005;23:47–55. [PubMed: 15637621]
2. Kleinman HK, Philp D, Hoffman MP. Role of the Extracellular Matrix in Morphogenesis. *Curr Opin Biotechnol* 2003;14:526–32. [PubMed: 14580584]
3. Stevens MM, George JH. Exploring and Engineering the Cell Surface Interface. *Science* 2005;310:1135–8. [PubMed: 16293749]
4. Behravesh E, Sikavitsas VI, Mikos AG. Quantification of Ligand Surface Concentration of Bulk-Modified Biomimetic Hydrogels. *Biomaterials* 2003;24:4365–74. [PubMed: 12922149]
5. Burdick JA, Anseth KS. Photoencapsulation of Osteoblasts in Injectable RGD-Modified PEG Hydrogels for Bone Tissue Engineering. *Biomaterials* 2002;23:4315–23. [PubMed: 12219821]

6. Weber LM, Hayda KN, Haskins K, Anseth KS. The Effects of Cell-Matrix Interactions on Encapsulated Beta-Cell Function within Hydrogels Functionalized with Matrix-Derived Adhesive Peptides. *Biomaterials* 2007;28:3004–11. [PubMed: 17391752]
7. Ifkovits JL, Burdick JA. Review: Photopolymerizable and Degradable Biomaterials for Tissue Engineering Applications. *Tissue Eng* 2007;13:2369–85. [PubMed: 17658993]
8. Hong Y, Legge RL, Zhang S, Chen P. Effect of Amino Acid Sequence and pH on Nanofiber Formation of Self-Assembling Peptides EAK16-II and EAK16-IV. *Biomacromolecules* 2003;4:1433–42. [PubMed: 12959616]
9. Zhang S. Emerging Biological Materials through Molecular Self-Assembly. *Biotechnol Adv* 2002;20:321–39. [PubMed: 14550019]
10. Zhang S. Fabrication of Novel Biomaterials through Molecular Self-Assembly. *Nat Biotechnol* 2003;21:1171–8. [PubMed: 14520402]
11. Jun HW, Paramonov SE, Hartgerink JD. Biomimetic Self-Assembled Nanofibers. *Soft Matter* 2006;2:177–181.
12. Hartgerink JD, Beniash E, Stupp SI. Self-Assembly and Mineralization of Peptide-Amphiphile Nanofibers. *Science* 2001;294:1684–8. [PubMed: 11721046]
13. Hartgerink JD, Beniash E, Stupp SI. Peptide-Amphiphile Nanofibers: A Versatile Scaffold for the Preparation of Self-Assembling Materials. *Proc Natl Acad Sci U S A* 2002;99:5133–8. [PubMed: 11929981]
14. Paramonov SE, Jun HW, Hartgerink JD. Self-Assembly of Peptide-Amphiphile Nanofibers: The Roles of Hydrogen Bonding and Amphiphilic Packing. *J Am Chem Soc* 2006;128:7291–8. [PubMed: 16734483]
15. Stendahl JC, Rao MS, Guler MO, Stupp SI. Intermolecular Forces in the Self-Assembly of Peptide Amphiphile Nanofibers. *Advanced Functional Materials* 2006;16:499–508.
16. Beniash E, Hartgerink JD, Storrer H, Stendahl JC, Stupp SI. Self-Assembling Peptide Amphiphile Nanofiber Matrices for Cell Entrapment. *Acta Biomater* 2005;1:387–97. [PubMed: 16701820]
17. Jun HW, Yuwono V, Paramonov SE, Hartgerink JD. Enzyme-Mediated Degradation of Peptide-Amphiphile Nanofiber Networks. *Advanced Materials* 2005;17:2612–2617.
18. Jiang H, Guler MO, Stupp SI. The Internal Structure of Self-Assembled Peptide Amphiphiles Nanofibers. *Soft Matter* 2007;3:454–462.
19. Anderson JM, Kushwaha M, Tambralli A, Bellis SL, Camata RP, Jun HW. Osteogenic Differentiation of Human Mesenchymal Stem Cells Directed by Extracellular Matrix-Mimicking Ligands in a Biomimetic Self-Assembled Peptide Amphiphile Nanomatrix. *Biomacromolecules*. 2009ASAP
20. Galler KM, Cavender A, Yuwono V, Dong H, Shi S, Schmalz G, Hartgerink JD, D'Souza RN. Self-Assembling Peptide Amphiphile Nanofibers as a Scaffold for Dental Stem Cells. *Tissue Eng Part A* 2008;14:2051–8. [PubMed: 18636949]
21. Hosseinkhani H, Hosseinkhani M, Khademhosseini A, Kobayashi H, Tabata Y. Enhanced Angiogenesis through Controlled Release of Basic Fibroblast Growth Factor from Peptide Amphiphile for Tissue Regeneration. *Biomaterials* 2006;27:5836–44. [PubMed: 16930687]
22. Hosseinkhani H, Hosseinkhani M, Tian F, Kobayashi H, Tabata Y. Osteogenic Differentiation of Mesenchymal Stem Cells in Self-Assembled Peptide-Amphiphile Nanofibers. *Biomaterials* 2006;27:4079–86. [PubMed: 16600365]
23. Huang Z, Sargeant TD, Hulvat JF, Mata A, Bringas P Jr, Koh CY, Stupp SI, Snead ML. Bioactive Nanofibers Instruct Cells to Proliferate and Differentiate during Enamel Regeneration. *J Bone Miner Res* 2008;23:1995–2006. [PubMed: 18665793]
24. Sargeant TD, Oppenheimer SM, Dunand DC, Stupp SI. Titanium Foam-Bioactive Nanofiber Hybrids for Bone Regeneration. *J Tissue Eng Regen Med* 2008;2:455–62. [PubMed: 18850672]
25. Silva GA, Czeisler C, Niece KL, Beniash E, Harrington DA, Kessler JA, Stupp SI. Selective Differentiation of Neural Progenitor Cells by High-Epitope Density Nanofibers. *Science* 2004;303:1352–5. [PubMed: 14739465]
26. Rehfeldt F, Engler AJ, Eckhardt A, Ahmed F, Discher DE. Cell Responses to the Mechanochemical Microenvironment--Implications for Regenerative Medicine and Drug Delivery. *Adv Drug Deliv Rev* 2007;59:1329–39. [PubMed: 17900747]

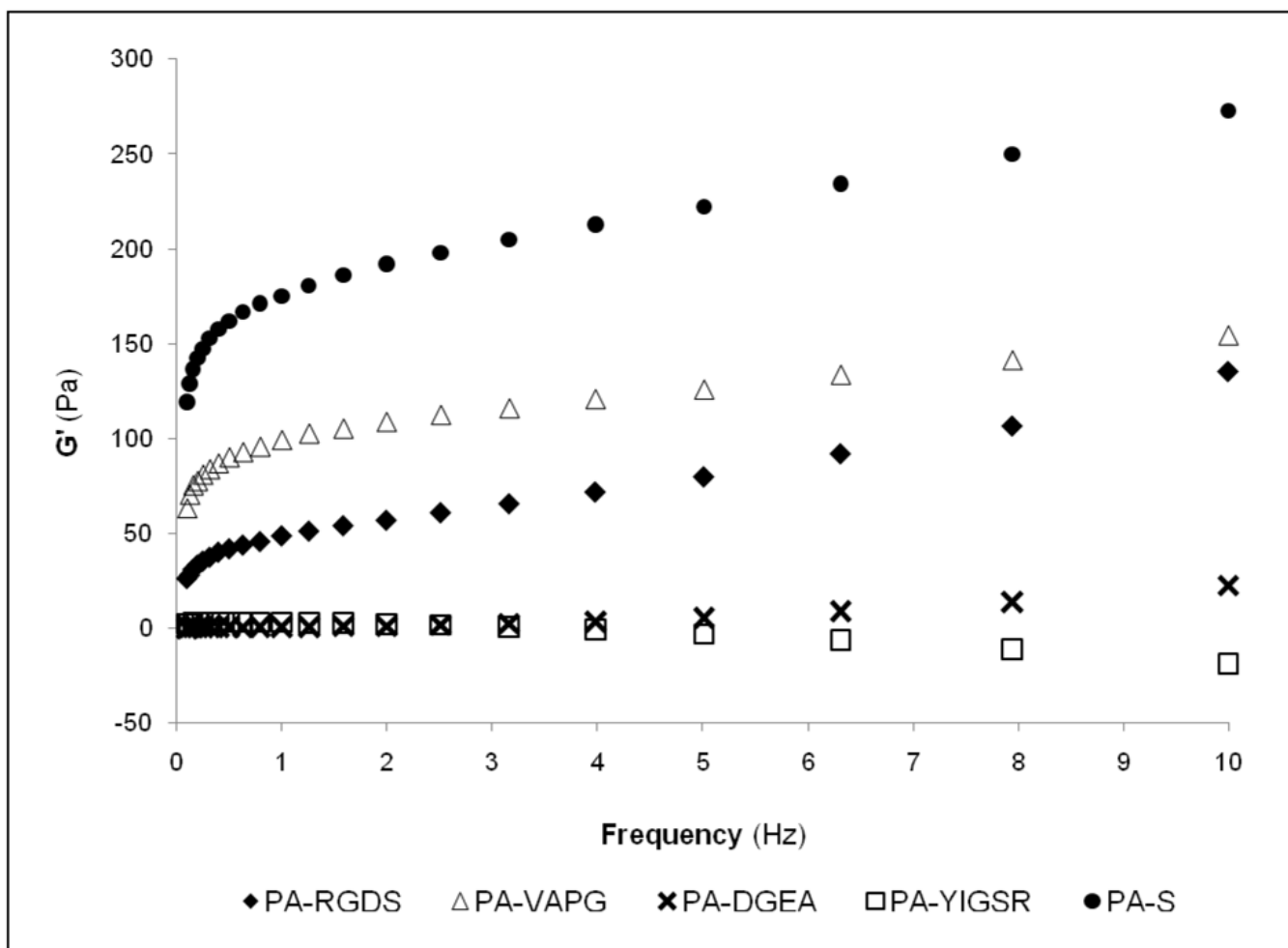


27. Discher DE, Janmey P, Wang YL. Tissue Cells Feel and Respond to the Stiffness of their Substrate. *Science* 2005;310:1139–43. [PubMed: 16293750]
28. Pelham RJ Jr, Wang Y. Cell Locomotion and Focal Adhesions are Regulated by Substrate Flexibility. *Proc Natl Acad Sci U S A* 1997;94:13661–5. [PubMed: 9391082]
29. Peyton SR, Putnam AJ. Extracellular Matrix Rigidity Governs Smooth Muscle Cell Motility in a Biphasic Fashion. *J Cell Physiol* 2005;204:198–209. [PubMed: 15669099]
30. Paramonov SE, Jun HW, Hartgerink JD. Modulation of Peptide-Amphiphile Nanofibers via Phospholipid Inclusions. *Biomacromolecules* 2006;7:24–6. [PubMed: 16398493]
31. Jung JP, Jones JL, Cronier SA, Collier JH. Modulating the Mechanical Properties of Self-Assembled Peptide Hydrogels via Native Chemical Ligation. *Biomaterials* 2008;29:2143–51. [PubMed: 18261790]
32. Behanna HA, Donners JJ, Gordon AC, Stupp SI. Coassembly of Amphiphiles with Opposite Peptide polarities into Nanofibers. *J Am Chem Soc* 2005;127:1193–200. [PubMed: 15669858]
33. Niece KL, Hartgerink JD, Donners JJ, Stupp SI. Self-Assembly Combining Two Bioactive Peptide-Amphiphile Molecules into Nanofibers by Electrostatic Attraction. *J Am Chem Soc* 2003;125:7146–7. [PubMed: 12797766]
34. Solis FJ, Stupp SI, de la Cruz MO. Charge induced pattern formation on surfaces: segregation in cylindrical micelles of cationic-anionic peptide-amphiphiles. *J Chem Phys* 2005;122:54905. [PubMed: 15740351]
35. Israelachvili JN, Mitchell DJ, Ninham BW. Theory of Self-Assembly of Lipid Bilayers and Vesicles. *Biochim Biophys Acta* 1977;470:185–201. [PubMed: 911827]
36. Hersel U, Dahmen C, Kessler H. RGD Modified Polymers: Biomaterials for Stimulated Cell Adhesion and Beyond. *Biomaterials* 2003;24:4385–415. [PubMed: 12922151]
37. Pierschbacher MD, Ruoslahti E. Cell Attachment Activity of Fibronectin can be Duplicated by Small Synthetic Fragments of the Molecule. *Nature* 1984;309:30–3. [PubMed: 6325925]
38. Gobin AS, West JL. Val-Ala-Pro-Gly, an Elastin-Derived Non-Integrin Ligand: Smooth Muscle Cell Adhesion and Specificity. *J Biomed Mater Res A* 2003;67:255–9. [PubMed: 14517884]
39. Harbers GM, Healy KE. The Effect of Ligand Type and Density on Osteoblast Adhesion, Proliferation, and Matrix Mineralization. *J Biomed Mater Res A* 2005;75:855–69. [PubMed: 16121356]
40. Massia SP, Hubbell JA. Human Endothelial Cell Interactions with Surface-Coupled Adhesion Peptides on a Nonadhesive Glass Substrate and Two Polymeric Biomaterials. *J Biomed Mater Res* 1991;25:223–42. [PubMed: 1829082]
41. Schnaper HW, Kleinman HK, Grant DS. Role of Laminin in Endothelial Cell Recognition and Differentiation. *Kidney Int* 1993;43:20–5. [PubMed: 8433560]
42. Meyers, MA.; Chawla, KK. *Mechanical Behavior of Materials*. Prentice Hall; Englewood Cliffs, NJ: 1998.
43. Mezger, TG. *The Rheology Handbook: for Users of Rotational and Oscillatory Rheometers*. Vol. 2. Vincentz Network; Hanover, Germany: 2006.
44. Nowak AP, Breedveld V, Pakstis L, Ozbas B, Pine DJ, Pochan D, Deming TJ. Rapidly recovering hydrogel scaffolds from self-assembling diblock copolypeptide amphiphiles. *Nature* 2002;417:424–8. [PubMed: 12024209]
45. Niece KL, Czeisler C, Sahni V, Tysseling-Mattiace V, Pashuck ET, Kessler JA, Stupp SI. Modification of Gelation Kinetics in Bioactive Peptide Amphiphiles. *Biomaterials* 2008;29:4501–9. [PubMed: 18774605]
46. Ingber DE. Tensegrity-Based Mechanosensing from Macro to Micro. *Prog Biophys Mol Biol* 2008;97:163–79. [PubMed: 18406455]
47. Engler AJ, Carag-Krieger C, Johnson CP, Raab M, Tang HY, Speicher DW, Sanger JW, Sanger JM, Discher DE. Embryonic Cardiomyocytes Beat Best on a Matrix with Heart-Like Elasticity: Scar-Like Rigidity Inhibits Beating. *J Cell Sci* 2008;121:3794–802. [PubMed: 18957515]
48. Engler AJ, Sen S, Sweeney HL, Discher DE. Matrix Elasticity Directs Stem Cell Lineage Specification. *Cell* 2006;126:677–89. [PubMed: 16923388]

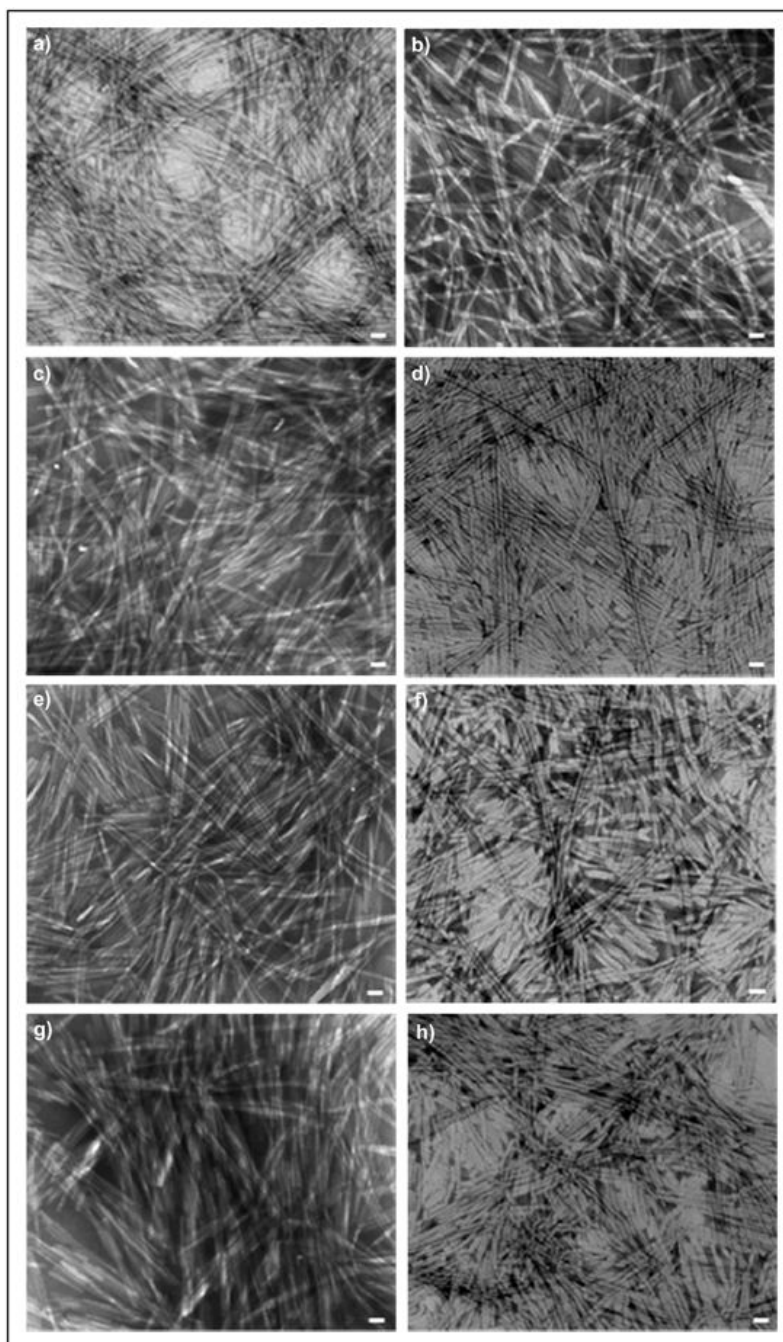
49. Hern DL, Hubbell JA. Incorporation of Adhesion Peptides into Nonadhesive Hydrogels Useful for Tissue Resurfacing. *J Biomed Mater Res* 1998;39:266–76. [PubMed: 9457557]
50. Koo LY, Irvine DJ, Mayes AM, Lauffenburger DA, Griffith LG. Co-Regulation of Cell Adhesion by Nanoscale RGD Organization and Mechanical Stimulus. *J Cell Sci* 2002;115:1423–33. [PubMed: 11896190]
51. Mann BK, West JL. Cell Adhesion Peptides Alter Smooth Muscle Cell Adhesion, Proliferation, Migration, and Matrix Protein Synthesis on Modified Surfaces and in Polymer Scaffolds. *J Biomed Mater Res* 2002;60:86–93. [PubMed: 11835163]
52. Palecek SP, Loftus JC, Ginsberg MH, Lauffenburger DA, Horwitz AF. Integrin-Ligand Binding Properties Govern Cell Migration Speed through Cell-Substratum Adhesiveness. *Nature* 1997;385:537–40. [PubMed: 9020360]
53. Kim JK, Anderson J, Jun HW, Repka MA, Jo S. Self-Assembling Peptide Amphiphile-Based Nanofiber Gel for Bioresponsive Cisplatin Delivery. *Mol Pharm* 2009;6:978–85. [PubMed: 19281184]
54. Tambralli A, Blakeney B, Anderson J, Kushwaha M, Andukuri A, Dean D, Jun HW. A Hybrid Biomimetic Scaffold Composed of Electrospun Polycaprolactone Nanofibers and Self-Assembled Peptide Amphiphile Nanofibers. *Biofabrication* 2009;1:025001.



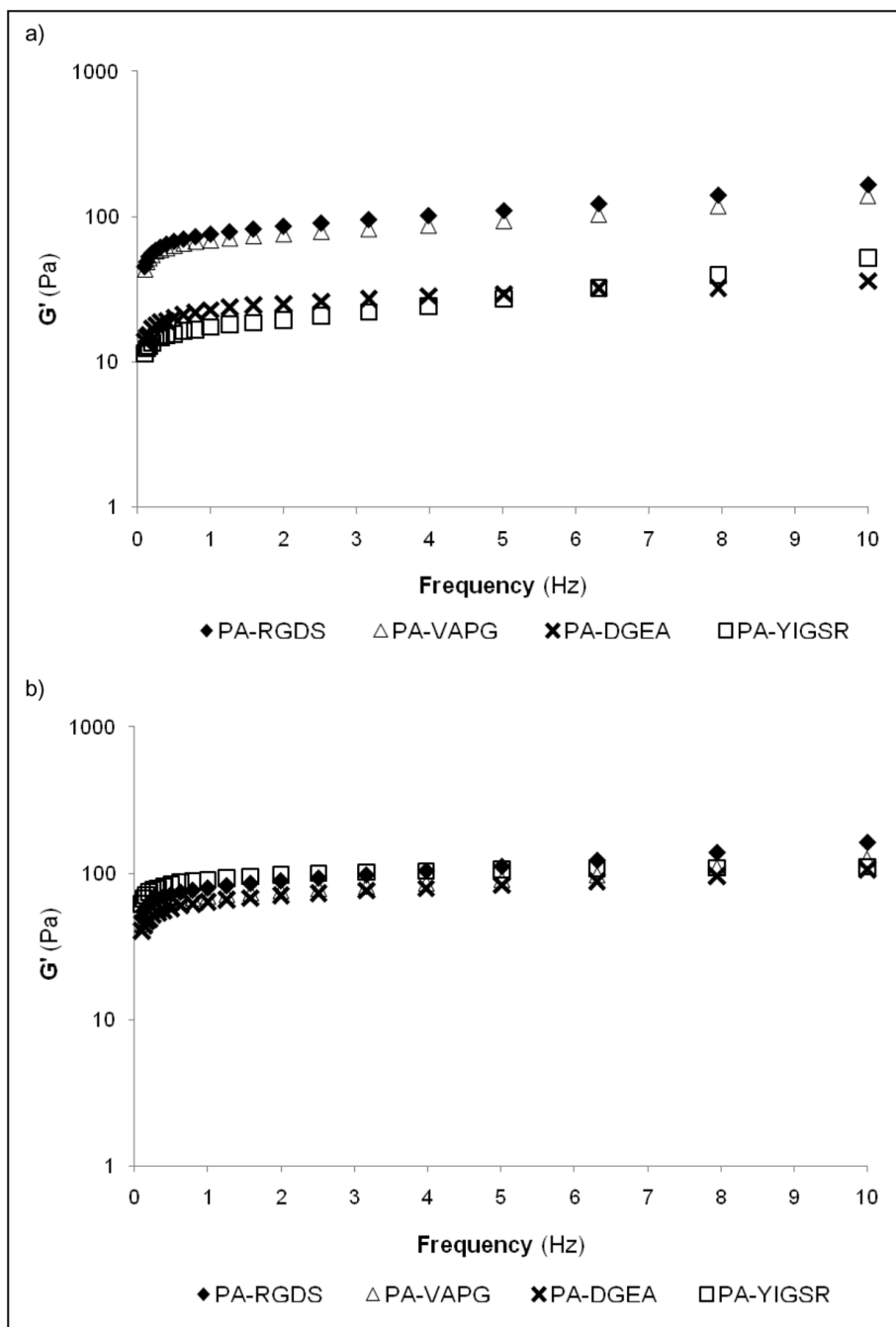
**Figure 1.** TEM images of the individually self-assembled PAs: (a) PA-RGDS, (b) PA-VAPG, (c) PA-DGEA, (d) PA-YIGSR, and (e) PA-S. Scale bar represents 20 nm.



**Figure 2.** Measure of storage modulus ( $G'$ ) over frequency using dynamic oscillatory rheometry. Individual PAs exhibited different viscoelastic properties after induced self-assembly.



**Figure 3.** TEM images of the functionalized PAs of (a,e) PA-RGDS, (b,f) PA-VAPG, (c,g) PA-DGEA, and (d,h) PA-YIGSR separately combined with PA-S at a molar ratio ( $M_r = PA/PA-S$ ) of (a–d) 1:1 or (e–h) 1:3. Scale bar represents 20 nm.





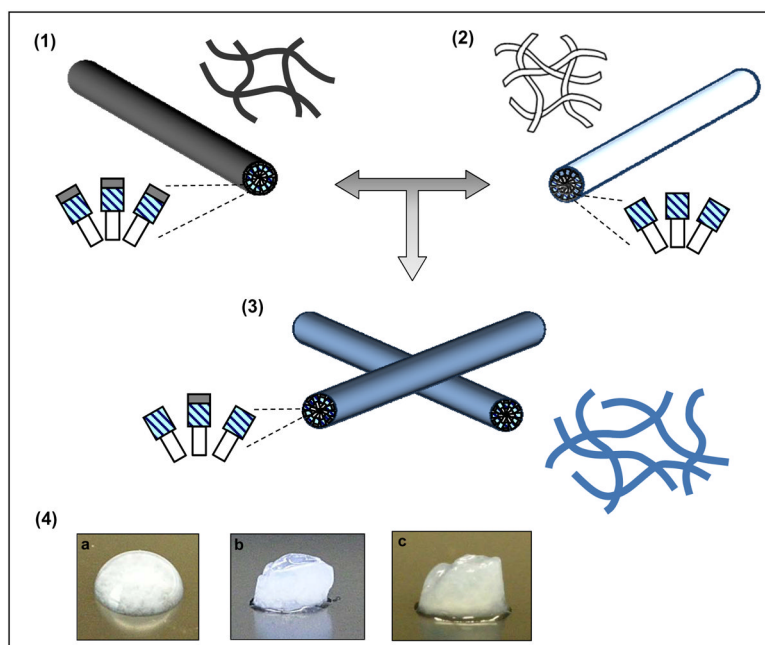










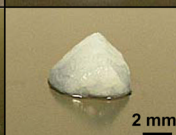
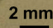
**Figure 4.** Storage moduli ( $G'$ ) of composite gels mixed with PA-S at different molar ratios. Individually combining the functionalized PAs with PA-S at a molar ratio ( $M_r = \text{PA}/\text{PA-S}$ ) of (a) 1:1 or (b) 1:3 stabilized viscoelasticity of the self-assembled gels.

**Scheme 1.**

Experimental design for combining (1,4a) functionalized PAs with (2,4b) PA-S at different molar ratios ( $M_r = \text{PA}/\text{PA-S}$ ) of 3:1, 1:1, or 1:3 to form (3,4c) self-assembled composite gels with greater controlled stability and maintained cell adhesive ligands.

**Table 1**

Modulating macroscopic gelation properties of peptide amphiphile composite hydrogels

	PA-RGDS	PA-VAPG	PA-DGEA	PA-YIGSR	PA-S
Molar ratio (PA/PA-S)	<i>Moderate gel</i>	<i>Moderate gel</i>	<i>Viscous solution</i>	<i>Viscous solution</i>	<i>Strong gel</i>
1:0 <sup>a</sup>					
<i>Improved gelation after combining with PA-S</i>					
1:1					
1:3					

<sup>a</sup> not mixed with any other PA solution before gelation



**Table 2**

Ratio of storage modulus to loss modulus for peptide amphiphile composite hydrogels

Molar ratio (PA/PA-S)	PA-RGDS	PA-VAPG	$G'/G''^a$	PA-DGEA	PA-YIGSR
1:0 <sup>b</sup>	4.17	5.94		3.54	4.03
3:1	4.29	6.28		3.25	4.03
1:1	4.57	6.21		4.43	6.25
1:3	5.83	7.05		5.21	6.52

<sup>a</sup> ratio of storage modulus ( $G'$ ) to loss modulus ( $G''$ ) at 1.26 Hz<sup>b</sup> not mixed with PA-S at Mr = 1:0